Calibration and Monte Carlo simulation of a single-photon counting charge-coupled device for single-shot X-ray spectrum measurements

Yonghong Yan (闫永宏)[1,2], Lai Wei (魏 来)[1], Xianlun Wen (温賢伦)[1], Yuchi Wu (吴玉迟)[1], Zongqing Zhao (赵宗清)[1], Bo Zhang (张 博)[1], Bin Zhu (朱 斌)[1], Wei Hong (洪 伟)[1], Leifeng Cao (曹磊峰)[1], Zeen Yao (姚泽恩)[2], and Yuqiu Gu (谷渝秋)[1*]

[1]*Science and Technology on Plasma Physics Laboratory, Research Center of Laser Fusion, China Academy of Engineering Physics, Mianyang 621900, China*

[2]*School of Nuclear Science and Technology, Lanzhou University, Lanzhou 730000, China*

[*]*Corresponding author: yqgu@caep.ac.cn*

Received April 15, 2013; accepted September 25, 2013; posted online November 6, 2013

A Princeton Instruments PI-LCX 1300 charge-coupled device (CCD) camera used for X-ray spectrum measurements in laser-plasma experiments is calibrated using three radioactive sources and investigated with the Monte Carlo code Geant4. The exposure level is controlled to make the CCD work in single photon counting mode. A summation algorithm for obtaining accurate X-ray spectra is developed to reconstruct the X-ray spectra, and the results show that the developed algorithm effectively reduces the low-energy tail caused by split pixel events. The obtained CCD energy response shows good linearity. The detection efficiency curves from both Monte Carlo simulations and the manufacturer agree well with the experimental results. This consistency demonstrates that event losses in charge collection processes are negligible when the developed summation algorithm of split pixel events is employed.

OCIS codes: 040.0040, 040.1880, 040.1520.

doi: 10.3788/COL201311.110401.

Laser-driven X-rays have attracted much interest because of the rapid development of ultra-intense laser-matter interaction[1−6]. Laser-produced X-rays, such as mono-energetic K lines[1] and continuous emission (bremsstrahlung and betatron)[3], have recently been extensively investigated. These X-rays are important in both fundamental and applied studies. K lines generated in ultra-intense laser-solid interactions facilitate the understanding of laser-plasma interactions[7,8] and can also be used as the backlighter for laser fusion studies[9]. Considered a novel X-ray source, the betatron X-ray emission from laser wake field acceleration has various potential applications, including contrast X-ray imaging[10]. Therefore, accurate spectrum measurements of these laser-produced X-rays are very important for their characterization. Charge-coupled devices (CCD) operated in single-photon counting mode have been widely applied in the characterization of laser-produced X-rays[11−14]. Analysis of data obtained from these devices is more straightforward compared with other spectrometers, e.g. crystal spectrometers[15,16].

In single-photon counting mode, the X-ray flux is attenuated to limit the exposure level to approximately one detected photon per 100 pixels. The readout count value of each pixel is proportional to the energy deposited by incident X-ray photons. Therefore, a histogram of the pixel value reproduces the incident X-ray spectrum. Prior to its application in laser-plasma experiments, the single-photon counting CCD should be thoroughly calibrated, including the energy response and detection efficiency, with standard X-ray sources (usually radioactive sources)[17]. Previous studies have reported the so-called split pixel event, in which the electron cloud generated by one incident X-ray photon spreads over several neighboring pixels[12,17]. Thus, an accurate algorithm is required to obtain the sum of the values of neighboring pixels that is proportional to the energy deposited by the incident photon.

In this letter, a CCD (PI-LCX 1300, Princeton Instruments, SA) with the measurement range from 2 to 30 keV was calibrated using three radioactive sources in the China National Institute of Metrology. We also simulated the X-ray photon transport in CCD chips using the Monte Carlo (MC) code Geant4[18]. A histogram algorithm was developed to reconstruct the X-ray spectrum, and the energy response and detection efficiency are consequently quantified. The obtained calibration results ensured accurate measurements in the X-ray experiments on the XingGuang-III laser facility at the China Academy of Engineering Physics.

The calibrated CCD has a 1340×1300 pixel array, pixel size of 20 × 20 (μm), and a 50-μm-deep depletion region. A 250-μm-thick beryllium (Be) in the front vacuum, which seals the unit for deep cooling, protects the CCD and reduces background by filtering low-energy X-rays. Three radioactive sources, namely, ^{55}Fe (5.89 keV), ^{241}Am (3.3, 13.95, and 17.54 keV), and ^{109}Cd (3.1, 22.16, and 24.9 keV) with activities of 65.4 ± 2.0, 53.5 ± 0.6, and 60.9 ± 1.1 kBq, respectively, were used to generate X-rays from 2 to 30 keV. One or more X-ray emission lines of each source were used. The exposure level was controlled by varying the integration time and the distance between the source and the CCD.

MC code Geant4 was used to simulate the X-ray transport in the CCD chips to obtain the energy deposition spectrum of incident X-ray photons from which the

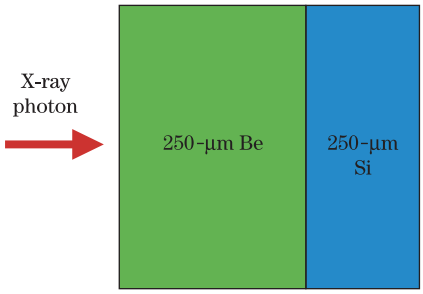

Fig. 1. (Color online) MC simulation model in Geant4 code.

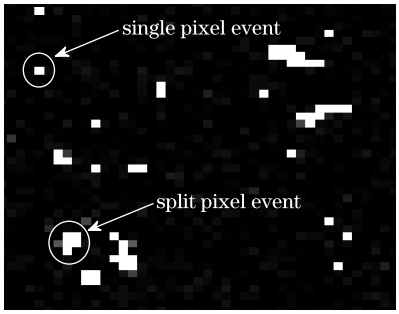

Fig. 2. Raw image from one CCD acquisition.

detection efficiency can be estimated. The simulation geometry model has a Si layer ($20 \times 20 \times 50$ (μm)) with a Be window ($20 \times 20 \times 250$ (μm)) in front that is set in the vacuum simulation environment (Fig. 1). X-ray photons (primary particles) are normally incident on the Be window. The deposited energy in the Si layer in each simulation event was recorded, and the histogram of the deposited energy served as the energy deposition spectrum corresponding to the spectrum measured in the actual experiment.

When the energy of an X-ray photon is deposited on the CCD chip, the charge cloud generated may be collected by a single pixel (single pixel event) or spread over several adjacent pixels (split pixel event). The latter occurs when an X-ray photon hits a pixel near its boundary. In addition, the so-called partial event phenomenon occurs when the X-rays hit the field-free region of the CCD array, wherein the charge cloud may not be collected completely, thereby causing a charge loss. A typical raw image obtained from one CCD acquisition experiment, from which single pixel events can be easily distinguished from split events, is shown in Fig. 2.

An algorithm was developed to treat the split pixel events to obtain a high-quality X-ray spectrum[19]. In this algorithm, a threshold, below which the pixel content was considered to be zero, was set to reduce the influence of thermal and electronic noise on the reconstructed spectra. A 3σ value of the raw histogram of a frame containing no signal (a noise histogram) was chosen as the threshold value, where σ is the standard deviation of the histogram. We first extracted the single pixel events and set the pixel value of these pixels to zero. Then, we obtained the sum of the pixel values of the two-, three-, four-, and multi-pixel (up to 15×15) events sequentially. The summed value of the multi-pixel events may be around 1, 2, 3 ... times of the single pixel event, since the pile-up events can occur in the summation processes. If the summed pixel value is around once of the single pixel event, then it is a split event of one photon. If the value is around twice the single pixel event, then it is a split event of two photons. Additionally, we accumulated two events at the location of the summed-pixel-value/2 in the spectrum. When the summed pixel value was around n times of the single pixel event, we considered this pixel event similar to the other events. Through this process, the split pixel events were well summed up, and their contribution to the spectrum was fully considered.

The reconstructed spectrum and raw histogram of X-rays emitted from ^{55}Fe are shown in Fig. 3. The raw spectrum has a large number of low-energy deposition events caused by the charge spread to more than one pixel (split pixel events). After correction using the developed summation algorithm, the low-energy events disappear in the reconstructed spectrum (blue line in Fig. 3), which contains both the single and split pixel events, and the number of events in the peak increase. Thus, the signal/noise ratio of the spectrum is enhanced. The developed algorithm adds the pile-up events to the main line in the reconstructed spectrum, so no pile-up event peak is observed in Fig. 3. This treatment is different from that in Ref. [12], in which a so-called cluster reconstruction-type algorithm was adopted to clearly define the two-photon region (the pile-up peak still exists). In principle, the reconstructed spectrum has a lower energy resolution than the spectrum containing single pixel events only because of the high reading noise from several pixels. Given the low-energy resolution, the escape peaks of the Si K line and the Mn K_β line are not obvious in the reconstructed spectrum.

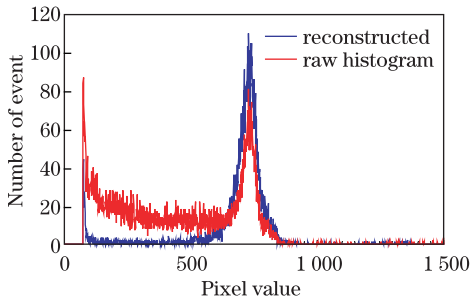

Fig. 3. (Color online) Raw histogram (red line) and reconstructed spectrum (blue line), including both single and split pixel events.

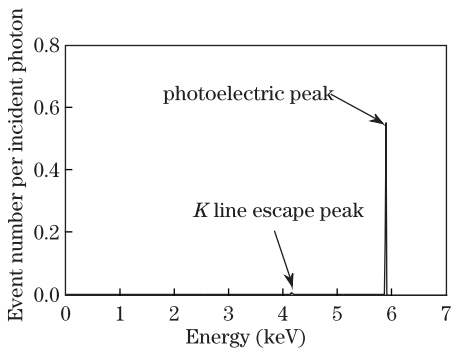

Fig. 4. Energy spectrum of 5.89-keV photon obtained by MC simulation.

The ^{55}Fe (5.89 keV) X-ray spectrum from the MC simulation is shown in Fig. 4. The spectrum is not broadened because of an unknown energy resolution function with photon energy. In addition to the photoelectric peak, the K line escape peaks of the Si element can also be observed. In the detection efficiency calculation, the number of detected photons is given by the counts contained in the photoelectric peak.

Seven X-ray lines from the radioactive sources mentioned above were used to obtain the CCD energy response. The results are shown in Fig. 5, in which the photon energy is observed to scale linearly with the CCD counts (readout pixel value). The counts for each energy point are determined to be the central value at the main peak in their respective energy spectra. A CCD pixel produces a count for every 8.1 eV of deposited energy. Therefore, for an unknown X-ray photon emitted from intense laser-plasma interactions, its energy can be determined according to the scaling shown in Fig. 5.

The detection efficiency of the CCD is

$$\eta = \frac{N_{\rm p}}{N_0} \times 100\%, \tag{1}$$

where $N_{\rm p}$ is the number of detected photons, and N_0 is the total number of photons incident on the CCD plane. In the experiments and simulations, N_p represents the event counts located in the main lines of the photon spectra, and the number of incident photons in the experiments can be calculated by

$$N_0 = At\frac{\Omega}{4\pi}IT, \tag{2}$$

where A is the source activity, t is the exposure time, Ω is the solid angle subtended by the CCD chip, I is the photon emission probability in one decay event of the radioactive source, and T is the transmission through the air. The source-to-CCD distance, which determines the solid angle subtended by the CCD chip, was 74.3±2.0 mm in all experiments. The exposure time for the ^{55} Fe source was 60.0±2.0 and 90.0±2.0 s for the ^{241} Am and ^{109} Cd source, considering the low detection efficiency of the high energy X-rays from the latter two sources.

The detection efficiency curves of the PI-LCX 1300 CCD is shown in Fig. 6. The MC simulation results and the data provided by the manufacturer are also presented, both of which agree well with the experimental

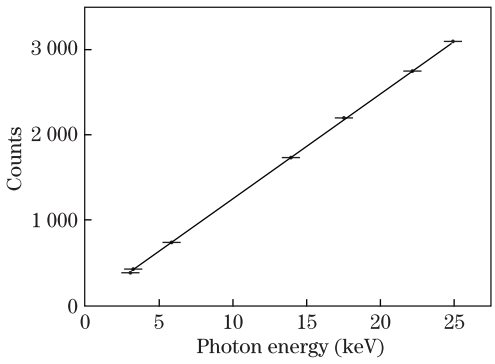

Fig. 5. Readout counts of the CCD versus photon energy. The fitted line gives 8.1 eV/count.

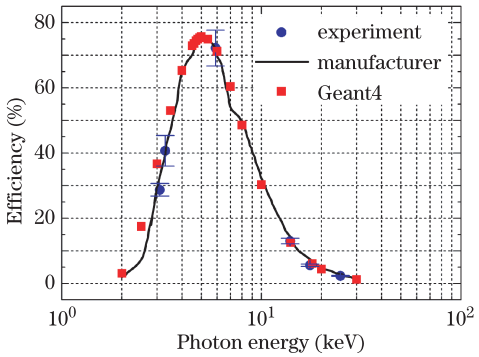

Fig. 6. (Color online) Detection efficiency versus X-ray photon energy.

results. From the MC simulation using Geant4 code, only the energy deposition is obtained, and it does not include the pair creation and charge collection process. In the experiments, the produced electron charges may not be collected completely, which may cause event losses in photoelectric peaks, resulting in decreased detection efficiency. However, the agreement between the simulation and experimental results indicates that event losses in charge collection processes are negligible when the developed summation algorithm is used.

As shown in Fig. 6, a peak in the detection efficiency curve can be observed, which is due to the Be window in front of the CCD chip. This phenomenon is caused by the absorption of the Be window of the low-energy photons, whereas the high-energy photons penetrate both the Be and the Si layers.

The CCD simulation results are consistent with the data from the specification provided by the manufacturer, except in the low-energy range ($<$ 4 keV), in which the simulation results are slightly higher than the results presented by the manufacturer. Additional simulations indicate that this discrepancy is due to the simulation of the X-ray absorption in a vacuum environment in the present study, whereas the manufacturer may have considered the X-ray absorption in air.

In conclusion, we calibrate and simulate a PI-LCX 1300 CCD that is used for X-ray measurements in ultra-intense laser-plasma experiments. The CCD is operated in single-photon counting mode by controlling the exposure level. The developed algorithm serves as an appropriate method for improving the X-ray spectrum. The energy response and detection efficiency of the CCD were obtained. The results provide basic information for the absolute determination of laser-produced X-rays on the XingGuang-III laser facility at the China Academy of Engineering Physics.

This work was supported by the National Natural Science Foundation of China (Nos. 10975121, 10905051, 10902051, and 11174259), the Foundation of CAEP (Nos. 2009A0102003 and 2011B0102021), and the Foundation of Science and Technology on Plasma Physics Laboratory (No. 9140C6802041004).

References

1. L. Chen, M. Kando, M. Xu, Y. Li, J. Koga, M. Chen, H. Xu, X. Yuan, Q. Dong, Z. Sheng, S. V. Bulanov, Y.

Kato, J. Zhang, and T. Tajima, Phys. Rev. Lett. **100,** 045004 (2008).

2. F. Dorchies, M. Harmand, D. Descamps, C. Fourment, S. Hulin, S. Petit, O. Peyrusse, and J. J. Santos, Appl. Phys. Lett. **93,** 121113 (2008).
3. S. Fourmaux, S. Corde, K. T. Phuoc, P. M. Leguay, S. Payeur, P. Lassonde, S. Gnedyuk, G. Lebrun, C. Fourment, V. Malka, S. Sebban, A. Rousse, and J. C. Kieffer, New J. Phys. **13,** 033017 (2011).
4. M. Schnell, A. Sävert, B. Landgraf, M. Reuter, M. Nicolai, O. Jäckel, C. Peth, T. Thiele, O. Jansen, A. Pukhov, O. Willi, M. C. Kaluza, and C. Spielmann, Phys. Rev. Lett. **108,** 075001 (2012).
5. G. R. Plateau, C. G. R. Geddes, D. B. Thorn, M. Chen, C. Benedetti, E. Esarey, A. J. Gonsalves, N. H. Matlis, K. Nakamura, C. B. Schroeder, S. Shiraishi, T. Sokollik, J. van Tilborg, C. Toth, S. Trotsenko, T. S. Kim, M. Battaglia, T. Stöhlker, and W. P. Leemans, Phys. Rev. Lett. **109,** 064802 (2012).
6. Y. Wu, Z. Zhao, B. Zhu, K. Dong, X. Wen, Y. He, Y. Gu, and B. Zhang, Chin. Opt. Lett. **10,** 063501 (2012).
7. K. Yasuike, M. H. Key, S. P. Hatchett, R. A. Snavely, and K. B. Wharton, Rev. Sci. Instrum. **72,** 1236 (2001).
8. P. M. Nilson, J. R. Davies, W. Theobald, P. A. Jaanimagi, C. Mileham, R. K. Jungquist, C. Stoeckl, I. A. Begishev, A. A. Solodov, J. F. Myatt, J. D. Zuegel, T. C. Sangster, R. Betti, and D. D. Meyerhofer, Phys. Rev. Lett. **108,** 085002 (2012).
9. H.-S. Park, D. M. Chambers, H.-K. Chung, R. J. Clarke, R. Eagleton, E. Giraldez, T. Goldsack, R. Heathcote, N. Izumi, M. H. Key, J. A. King, J. A. Koch, O. L. Landen, A. Nikroo, P. K. Patel, D. F. Price, B. A. Remington, H. F. Robey, R. A. Snavely, D. A. Steinman, R. B. Stephens, C. Stoeckl, M. Storm, M. Tabak, W. Theobald, R. P. J. Town, J. E. Wickersham, and B. B. Zhang, Phys. Plasmas **13,** 056309 (2006).
10. S. Fourmaux, S. Corde, K. T. Phuoc, P. Lassonde, G. Lebrun, S. Payeur, F. Martin, S. Sebban, V. Malka, A. Rousse, and J. C. Kieffer, Opt. Lett. **36,** 2426 (2011).
11. C. Stoeckl, W. Theobald, T. C. Sangster, M. H. Key, P. Patel, B. B. Zhang, R. Clarke, S. Karsch, and P. Norreys, Rev. Sci. Instrum. **75,** 3705 (2004).
12. C. Fourment, N. Arazam, C. Bonte, T. Caillaud, D. Descamps, F. Dorchies, M. Harmand, S. Hulin, S. Petit, and J. J. Santos, Rev. Sci. Instrum. **80,** 083505 (2009).
13. W. Fullagar, J. Uhlig, M. Walczak, S. Canton, and V. Sundstrom, Rev. Sci. Instrum. **79,** 103302 (2008).
14. D. B. Thorn, C. G. R. Geddes, N. H. Matlis, G. R. Plateau, E. H. Esarey, M. Battaglia, C. B. Schroeder, S. Shiraishi, T. Stohlker, C. Toth, and W. P. Leemans, Rev. Sci. Instrum. **81,** 10E325 (2010).
15. W. Theobald, C. Stoeckl, P. A. Jaanimagi, P. M. Nilson, and M. Storm, Rev. Sci. Instrum. **80,** 083501 (2009).
16. J. F. Seely, C. A. Back, C. Constantin, R. W. Lee, H. K. Chung, L. T. Hudson, C. I. Szabo, A. Henins, G. E. Holland, R. Atkin, and L. Marlin, J. Quant. Spectrosc. Ra. **99,** 572 (2006).
17. B. R. Maddox, H. S. Park, B. A. Remington, and M. McKernan, Rev. Sci. Instrum. **79,** 10E924 (2008).
18. S. Agostinelli, J. Allison, K. Amako, J. Apostolakis, H. Araujo, P. Arce, M. Asai, D. Axen, S. Banerjee, G. Barrand, F. Behner, L. Bellagamba, J. Boudreau, L. Broglia, A. Brunengo, H. Burkhardt, S. Chauvie, J. Chuma, R. Chytracek, G. Cooperman, G. Cosmo, P. Degtyarenko, A. Dell'Acqua, G. Depaola, D. Dietrich, R. Enami, A. Feliciello, C. Ferguson, H. Fesefeldt, G. Folger, F. Foppiano, A. Forti, S. Garelli, S. Giani, R. Giannitrapani, D. Gibin, J. J. Gómez Cadenas, I. González, G. Gracia Abril, G. Greeniaus, W. Greiner, V. Grichine, A. Grossheim, S. Guatelli, P. Gumplinger, R. Hamatsu, K. Hashimoto, H. Hasui, A. Heikkinen, A. Howard, V. Ivanchenko, A. Johnson, F. W. Jones, J. Kallenbach, N. Kanaya, M. Kawabata, Y. Kawabata, M. Kawaguti, S. Kelner, P. Kent, A. Kimura, T. Kodama, R. Kokoulin, M. Kossov, H. Kurashige, E. Lamanna, T. Lampén, V. Lara, V. Lefebure, F. Lei, M. Liendl, W. Lockman, F. Longo, S. Magni, M. Maire, E. Medernach, K. Minamimoto, P. Mora de Freitas, Y. Morita, K. Murakami, M. Nagamatu, R. Nartallo, P. Nieminen, T. Nishimura, K. Ohtsubo, M. Okamura, S. O'Neale, Y. Oohata, K. Paech, J. Perl, A. Pfeiffer, M. G. Pia, F. Ranjard, A. Rybin, S. Sadilov, E. Di Salvo, G. Santin, T. Sasaki, N. Savvas, Y. Sawada, S. Scherer, S. Sei, V. Sirotenko, D. Smith, N. Starkov, H. Stoecker, J. Sulkimo, M. Takahata, S. Tanaka, E. Tcherniaev, E. Safai Tehrani, M. Tropeano, P. Truscott, H. Uno, L. Urban, P. Urban, M. Verderi, A. Walkden, W. Wander, H. Weber, J. P. Wellisch, T. Wenaus, D. C. Williams, D. Wright, T. Yamada, H. Yoshida, and D. Zschiesche, Nucl. Instrum. Methods Phys. Res. A **506,** 250 (2003).
19. L. Wei, Y. Yan, X. Wen, and Y. Gu, "Development of a summation algorithm for X-ray spectrum reconstruction in single photon counting charge-coupled devices data analysis" to be submitted. (2013).